2020

Robust placement and sizing of charging stations from a novel graph theoretic perspective

Hossein Parastvand
Edith Cowan University

Octavian Bass
Edith Cowan University

Mohammad A. S. Masoum

Airlie Chapman

Stefan Lachowicz
Edith Cowan University

10.1109/ACCESS.2020.3005677
Parastvand, H., Bass, O., Masoum, M. A. S., Chapman, A., & Lachowicz, S. (2020). Robust Placement and Sizing of Charging Stations from a Novel Graph Theoretic Perspective. *IEEE Access, 8,* 118593-118602. https://doi.org/10.1109/ACCESS.2020.3005677

IEEE Access
Multidisciplinary : Rapid Review : Open Access Journal

Received May 17, 2020, accepted June 25, 2020, date of publication June 29, 2020, date of current version July 8, 2020.

Digital Object Identifier 10.1109/ACCESS.2020.3005677

Robust Placement and Sizing of Charging Stations From a Novel Graph Theoretic Perspective

HOSSEIN PARASTVAND[1], (Student Member, IEEE), OCTAVIAN BASS[1], (Senior Member, IEEE), MOHAMMAD A. S. MASOUM[2], (Senior Member, IEEE), AIRLIE CHAPMAN[3], (Senior Member, IEEE), AND STEFAN W. LACHOWICZ[1], (Senior Member, IEEE)

[1]Smart Energy Systems Research Group, School of Engineering, Edith Cowan University, Joondalup, WA 6027, Australia
[2]Department of Engineering, Utah Valley University, Orem, UT 84058, USA
[3]Department of Mechanical Engineering, School of Engineering, The University of Melbourne, Melbourne, VIC 3010, Australia

Corresponding author: Hossein Parastvand (h.parastvand@ecu.edu.au)

This work was supported by Edith Cowan University Open Access Funding Support Scheme.

ABSTRACT This paper proposes analytical approaches to extend the capacity of existing networks of electric vehicles (EVs) by placement of additional charging stations (CSs) as well as determining the sizes of existing and new CSs in order to handle future expansions of EVs. The EV flow at CSs is modeled by a graph where nodes are potential locations for CSs and edges are uncertain parameters representing the variable EV flow at CSs. The required extra CS locations are explored by transforming the CS placement problem into a controllability framework addressed by maximum matching principle (MMP). To find the sizes of each CS, the graph of CS network is partitioned featuring only one CS in each subgraph. The size of CS in each subgraph is then determined by transforming the problem into the problem of robust stability of a system with uncertain parameters where each parameter is associated with an edge of subgraph. The zero exclusion principle is then tested for the related Kharitonov rectangles and polygonal polynomials of closed loop system with selected feedback gain as CS capacity. The proposed analytical approach is tested on the existing Tesla CS Network of Sydney. The locations of extra required CSs as well as the sizes of existing and new CSs are determined to maintain the waiting times at all stations below the threshold level.

INDEX TERMS Electric vehicle, charging station, placement, sizing, fast charging, graph theory.

I. INTRODUCTION

A esponse to the greenhouse gases emissions, the internal combustion vehicles have been replacing rapidly by electrically powered vehicles. As such, the charging infrastructures, mainly charging stations (CSs), have always been expanded in order to supply the ever increasing demand of new EVs added to the network.

The optimization techniques are the focal point of methodologies related to EV problems (for example see [1], [13]). Some of the most frequently used optimization techniques in literature addressing various EV related problems include Monte Carlo simulation [3], [4], Grasshooper optimization algorithm [5], particle swarm optimization (PSO) [6], [7], CPLEX [8], [9], genetic algorithm [10], active-set algorithm [11], and K-means cluster [12]. The Markov and Monte Carlo simulation are used in [3] and [4] to model the urban driving cycle and to simulate the EV travel patterns and charging demand, respectively. Grasshopper optimization is used in [5] to address the sizing of CSs while the optimal placement of distributed generations and shunt capacitors are also investigated. In [6], a multi-objective PSO and geographic information system are used for the planning of CSs with a focus on the underlying economic impacts. PSO is also used in [7] for dynamic economic emission dispatch with load demand management where a large penetration during crest-and-valley is considered. The CPLEX solver is used in [8] to construct an integer linear program in order to address the EV salesman problem constrained to a predefined windows of waiting times. CPLEX is also implemented in [9] to attain a mixed-integer linear program model for stochastic scheduling of plug-in electric vehicles (PEVs) aggregator in day-ahead and reserve market. A review on energy management and optimization of EVs based on genetic algorithm is presented

The associate editor coordinating the review of this manuscript and approving it for publication was Zhan Bu.

in [10]. Using active-set algorithm in [11], a framework is proposed to optimally deploy various types of CSs where a heuristic algorithm is implemented for solving the model. The EV network of China is divided into 31 provinces by k-means cluster [12] to investigate the impact of EVs on the greenhouse gas emissions.

One of the main focus of studies related to EV networks during the last few years has been the Optimal placement and sizing of CSs in order to maintain the waiting time below a threshold level ([5]- [6], and [12]- [14]) where a sort of optimization technique is used in almost all of the proposed approach. The optimization techniques implemented for EV problems usually suffer from computational issues such as complexity and intractable solution [13]. On the other hand, almost all (if not all) previous studies have addressed the CS placement problems for regions where there are no existing CSs. However, as the EV networks are rapidly growing, there is a need for placement and sizing of new stations while also the existing CSs must be re-sized.

A novel approach to CS placement and sizing is proposed in [14] which, unlike the majority of current approaches based on optimization techniques, relies on graph theoretic properties of the graph of EV networks. It transforms the CS placement to the problem of finding the set of required driver nodes for CN controllability using the exact controllability method (ECM). Similarly, the CS sizing problem is transformed to the problem of finding a linear quadratic regulator (LQR) for each partition of EV network. However, there are some limitations for this approach. It lacks the consideration of dynamic traffic flow during the day and only relies on 17 instances of traffic flow. Moreover, the proposed CS placement approach can not be applied for networks where there are some pre-existing CSs.

To address the above challenges, we have developed the control framework first introduced in [14] in order to address the CS placement and sizing for a network with existing CSs and variable flow of EVs. Firstly, the mathematical model of the underlying graph of EV network is improved by separating the traffic flow at individual node from the trafic flow between nodes. The proposed approach then transforms the placement and sizing problems to controllability and feedback gain design problems where the system states are the waiting times at CSs and control inputs are the charging capacity supplied via driver nodes acting as CSs. A model of underlying EV network is constructed using a graph where nodes are the potential locations of CSs and edges link two nearby nodes where the weights of edges represent the number of EVs in the area. The ECM implemented in [14] is not applicable for CS placements in networks with existing CSs. Thus we use another graph theoretic property, known as maximum matching principle, by modifying it to a case where there are some pre-set unmatched nodes, and then the locations of new CSs are determined by finding the remaining unmatched nodes on the graph of CS network. Moreover, the proposed approach in [14] determines the locations and sizes of CSs according to a static EV flow corresponding to few traffic instances during the day, while in this paper, the control framework and the graph theoretic approach of [14] are adapted to a more general and practical case that considers variable traffic flow. Throughout the paper, the term "traffic flow" refers to the flow of EVs at the charging stations. It is represented by uncertain parameters with known maximum and minimum values assigned to the weight of each edge.

To locate the number and locations of additional CSs, we determine the driver nodes for the associated graph of EV network based on the maximum matching principal while considering the weights of edges as an interval uncertain parameter. To address the sizing problem of existing and new CSs, we first partition the graph of EV network featuring only one CS (from the set of CSs located from the solution of CS placement) in each subgraph. Then, we use the Kharitanov theorem and zero exclusion condition [15] to transform the CS sizing problem to zero exclusion of the Kharitonov rectangles or polygonal polynomials of the closed loop system attained from the sub-graphs (or the problem of robust stability of plants with uncertain parameters [16]). Detailed simulations and analyses of the Tesla CS network of Sydney verify that the proposed approach has significant impact on reducing the waiting times at CSs in Year 2025 assuming 500% increase in EV traffic [19]. The main contributions of this paper (in general and compared to [14]) are:

1) Unlike the usual optimization methods, the proposed approaches are analytic, computationally effective, and rely on established concepts from graph/control theories.
2) The mathematical model of the EV network proposed in [14] is improved by separating the impacts of traffic flows at nodes and between nodes.
3) We consider the CS placement and sizing for expanding EV networks with existing CSs. As the best of authors' knowledge, there is no analytic approach to placement of new CSs for an expanding network considering the future traffic.
4) The ECM method used in [14] is not applicable to CS placement for expanding networks. Here, we modify the MMP so that it can be used for placement of CSs when there are some pre-existing CSs.
5) We consider and model the dynamic of traffic flow using interval uncertain parameters.
6) The proposed approach is able to maintain the waiting times at CSs below a threshold level in the presence of variable traffic.
7) The proposed approach in this paper can be easily implemented to any EV network with variable traffic. The only required data is the model of the underlying graph and the maximum/minimum number of EVs arriving at CSs during operation.

The rest of the paper is organized as follows. Section II develops an EV network model based on graph theory followed by new approaches for robust CS placement and sizing

of existing and new CSs. Section IV presents and analyzes comprehensive simulation results for the existing Tesla CS network of Sydney, Australia, followed by conclusions.

II. CS PLACEMENT AND SIZING FOR EXPANDING EV NETWORKS WITH VARIABLE TRAFFIC FLOW AT CSs

In this section, the modeling of the CS network based on graph theory is explained followed by a new approach for the placement and sizing of existing and new CSs that considers the variable traffic flows of the EV network.

A. GRAPH-THEORETIC MODELING OF EV NETWORK

Graph theory [17] is one of the bases of the mathematical analysis in this study. Here, the terms graph or network are reserved for the abstract mathematical model of the composition of nodes and edges of CS network where nodes are the potential locations of CSs and edges are the traffic flow between nearby nodes. The weights of edges represent the traffic or the number of vehicles. A graph is defined as the pair $\mathcal{G} = (V, E)$ where V and E are the finite set of nodes and edges of the graph, respectively.

The worldwide locations and sizes of the existing charging stations are accessible through various CS networks and maps such as the Tesla CS, Plug In America, Go Electric Stations, Open Charge Map, Plug Surfing, EV Charger Maps, LEMnet, POP Point, Sun Country Highway and PlugShare. For the molding, formulation, simulations and analyses of this paper, we use the Tesla CS Map of Sydney, Australia [18]. Assuming 500% increase in Sydney EV traffic by Year 2025 [19], this model is augmented by adding some virtual candidate locations (nodes) for additional CSs at various spots across the map to construct the graph of the whole network. Although, the simulation is performed for this specific network, it can be easily implemented to all EV networks with variable traffic.

Considering the waiting times at all potential and existing locations of CSs as the states of system and assuming that there is an online tool presenting the instance waiting times to the drivers and the majority of drivers prefer a CS with a low waiting time in nearby area, the dynamic equation

$$T_i = T_{i_0} + \int_0^t W_{ch} T_{ch} q_{ii}(t)dt + \sum_{j=1}^{n} q_{ij} a_{ij} T_j, \; i = 1, \ldots, n \tag{1}$$

governs the dynamics of waiting times at all nodes. In 1, T_i is the state of i^{th} node, T_{i0} is the initial state of node i, W_{ch} is the ratio of charge to full charge, T_{ch} is the full charging time, $q_{ii}(t)$ is the uncertain flow of EVs at node i, q_{ij} is the uncertain flow of EVs between nodes i and j, a_{ij} is the outer coupling matrix in which $a_{ij} = 1$ if there is an edge between nodes i and j but $a_{ij} = 0$ otherwise, T_j represents the adjacent nodes to node i, and n is the number of nodes. Given $\int_0^t q_{ii}(t)dt = Q_{ii}(t)$, we can write

$$\begin{aligned} \dot{T}_i &= W_{ch} T_{ch} Q_{ii} dt + \sum_{j=1}^{n} q_{ij} a_{ij} T_j, \quad i = 1, \ldots, n \\ \dot{Q}_{ii} &= q_{ii}. \end{aligned} \tag{2}$$

Equation 2 governs the dynamics of waiting times T_i at all nodes since when the drivers are consciously choose a target CS, then all states T_i, $i = 1, 2, \ldots, n$, incrementally converge to nearly equal final states. Equation (2) simulates the waiting times when no CS exists and thus the waiting times increase constantly. To maintain all waiting times reasonably below a threshold level, a controlling term must be added to (2) which pins a few nodes to act as CSs in order to inject the control signal (charging supply) to the network. Considering the sizes of CSs as the values of control inputs of the system, the governing equation of CS network can be written as

$$\dot{T}_i = T_i + \sum_{j=1}^{n} q_{ij} a_{ij} H T_j - \delta B u_i, \quad i = 1, \ldots, n \tag{3}$$

where u_i is the control signal or charging supply injected through the CS at node i, B is the input matrix, and $\delta_i = 1$ if node i is selected as a CS and $[\delta_i] = 0$ otherwise. Equation (3) facilitates transforming the CS sizing problem to a control framework in which finding the control signal is equivalent to finding the charging capacity required to maintain the state of system (3) or waiting times below a threshold level.

B. GRAPH-THEORETIC CS PLACEMENT IN EV NETWORKS WITH EXISTING CSs AND VARIABLE TRAFFIC

As verified in [14], the problem of CS placement can be transformed to the problem of finding the required driver nodes for the underlying graph of EV network where nodes are the potential places for CSs and edges represent the traffic flow (the flow of EVs at CSs) between two nearby nodes. System states are also defined as the waiting times T_i at each node i. The set of driver nodes are located in [14] by the exact controllability method which is based on the maximum geometric multiplicity of all eigenvalues of the system matrix. However, this method is not applicable here as a set of predetermined CSs are already placed. We use and modify an alternative method, known as maximum matching principle, to find the set of required driver nodes. Throughout the paper, the terms driver node, charging station, and CS have been used interchangeably, but they convey the same meaning.

Definition 1: For a graph $\mathcal{G}(V, E)$, a matching M in $\mathcal{G}$ is a set of pairwise non-adjacent edges, none of which are loops, that is, there is no shared endpoints for none of edges or, equivalently, no two edges share a common node. A node is matched if it is an endpoint of one of the matching set, otherwise, it is unmatched. Maximum matching M_{max} of the graph $\mathcal{G}$ is a matching of maximum size among all matchings in the graph.

The relation between maximum matching and controllability is first revealed in [22] where the Controllability of complex networks is attributed to the number of required driver nodes. Once the maximum set of matched nodes are identified, all unmatched nodes are considered as the set of driver nodes [22] needed to completely control the entire network. Considering (3) as a complex network with a set

of pre-existing CSs, the objective is to place a set of extra CSs to address future network expansion. Thus, here, the EV network is called "controllable" if we can drive the the states (waiting times) of (3) below a threshold level using a set of pre-existing and extra CSs. We first set the existing CSs as unmatched nodes and then attain the number and locations of extra CSs for (3) by modifying the maximum matching principle as summarized in proposition below.

Proposition 2: A given expanded graph $\mathcal{G}$ of a CS network with V nodes and existing set of driver nodes S^0_{CS} is controllable if the set of driver nodes is

$$S_{CS} = \{V| \; (V \in S^0_{CS}) \cup (V \in S^E_{SC})\} \tag{4}$$

where

$$S^E_{SC} = \{V| \; (V \notin M_{max}) \,\&\, (V \notin S^0_{CS})\}. \tag{5}$$

Proof: The proof is a straightforward result of computing the extra set of nodes S^E_{SC} using the maximum matching principle on the graph assuming that the set of nodes in S^0_{CS} are reserved as unmatched. □

Using the above proposition and the control framework of placement problem, the set of extra CSs can be found. Example below clarifies the implementation of the modified MMP for EV network.

Example 3: Figure 1 illustrates the implementation of the modified MMP on a subgraph of an EV network. It represent an existing CS at node 3 in Figure 1.a which is set as an unmatched node. The modified MMP has resulted in two matched edges indicated by red lines and one unmatched node (node 5) indicated by the red location symbol in Figure 1.b. Thus, the subgraph will have two CSs, one pre-existing and one added.

In Section III, the placement of required extra CSs for the expanded Tesla CS network of Sydney, Australia is performed using this method.

C. GRAPH-THEORETIC SIZING OF NEW AND EXISTING CSs IN EV NETWORKS WITH VARIABLE TRAFFIC

To find the sizes of all CSs, first, we partition the CS graph into N_D subgraphs where there is only one CS (from the set of CSs attained from the solution of CS placement) in each subgraph. The partitioning algorithm decomposes the graph into N_D subgraphs which will be refined later by aiming at the final decomposition with as fewer interconnections as possible (see [20] for further details on the partitioning approach). Once the graph is partitioned, the corresponding dynamic of each subgraph similar to (3) is calculated in which B has only one non-zero entry corresponding to a node where a CS is placed. The state space representation of each subgraph can then be written as:

$$\dot{\mathbf{T}} = \mathcal{L}\mathbf{T} + B\mathbf{u} \;, y = CT \tag{6}$$

where $\mathcal{L} = \mathcal{D} - \sum_{j=1}^{n_s}(T_i - T_j)$, $i = 1, \ldots, n_s$, n_s is the number of nodes within the subgraph, $\mathcal{D}$ is the degree matrix, and $C = \mathbf{1}$. The state space representation of the subgraph in (6) can then be written as the transfer function

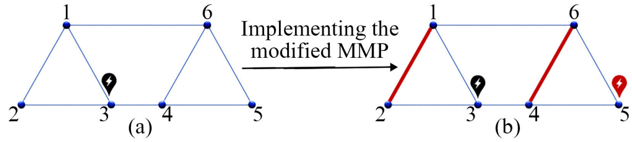

FIGURE 1. (a) A subgraph of EV network with an existing CS at node 3 and, (b) the implementation of the modified MMP which has resulted to two matched edges indicated by red lines and one added CS at node 5.

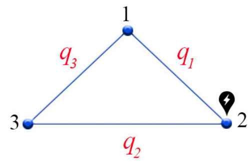

FIGURE 2. A graph with three uncertain edges and one CS.

$$G(s) = C(SI - L)^{-1}B \tag{7}$$

which is the Laplacian form of system (6).

The dynamic equation (7) for each subgraph is a transfer function $G(s) = \frac{N(s)}{D(s)}$ where both $N(s)$ and $D(s)$ are affine-linear uncertain polynomials. This is clarified by the following example.

Example 4: Consider the simple graph of Figure 2 with three nodes and one CS at node 2. The number of vehicles on the three edges are defined as $1 \leq q_1 \leq 10$, $1 \leq q_2 \leq 15$, and $1 \leq q_3 \leq 20$. Let $q_{ii} = 0$ and $q_{ij} = q_{ji}$ for $i = 1, 2, 3$. The Laplacian matrix of this network can be written as:

$$\mathcal{L} = \begin{bmatrix} 2 & -q_1 & -q_3 \\ -q_1 & 2 & -q_2 \\ -q_3 & -q_2 & 2 \end{bmatrix}, \quad C = \mathbf{1}, \quad B = [0\;1\;0]^T$$

The closed loop transfer function (7) with fixed controller k can then be written as

$$H(s) = \frac{k.N(s)}{D(s) + k.N(s)}$$

where $N(s) = s^2 + (-4 - q_1 - q_2)s + 4 + 2q_1 + q_2^2 - q_3^2 + 2q_2 + q_1q_3$ *and*

$$\begin{aligned} &D(s) + k.N(s) \\ &= s^3 + (-6 - kq_1 - 4k - kq_2)s^2 + s(4 - q_1^2 \\ &\quad - q_2^2 + 2kq_1 + kq_2^2 + 4k - kq_3^2 + 2kq_2 + kq_1q_3) + 2q_1^2 \\ &\quad + 4q_2^2 - 8 + 2kq_1 + kq_2^2 + 4k - kq_3^2 + 2kq_2 + kq_1q_3. \end{aligned}$$

The uncertainties of this non-linear polynomial can be over-bounded to construct an affine-linear uncertain polynomial. By defining new variables $Q_1 = kq_1$, $Q_2 = kq_2$, $Q_3 = q_1^2$, $Q_4 = q_2^2$, $Q_5 = kq_2^2$, $Q_6 = kq_3^2$ and $Q_7 = kq_1q_3$, the over-bounding polynomial can be written as

$$\begin{aligned} &D(s) + k.N(s) \\ &= s^3 + (-6 - Q_1 - 4k - Q - 2)s^2 \end{aligned}$$

$$+s(4-Q_3-Q_4+2Q_1+Q_5+4k-Q_6+2Q_2+Q_7)$$
$$+2Q_3+4Q_4-8+2q_1+Q_5+4k-Q_6+2Q_2+Q_7$$

which has an affine-linear uncertainty structure with uncertainty bounds $k \leq Q_1 \leq 10k$, $k \leq Q_2 \leq 15k$, $1 \leq Q_3 \leq 100$, $1 \leq Q_4 \leq 225$, $k \leq Q_5 \leq 225k$, $k \leq Q_6 \leq 400k$, *and* $k \leq Q_7 \leq 150k$.

As explained, the subsequent subgraphs of the CS network have affine-linear uncertain polynomials in the nominator and denominator of the related transfer functions. Each subgraph with an associated CS can be seen as a control system with unity feedback and a fixed compensator k that represents the charging capacity. The closed loop polynomial with fixed k can thus be seen as an affine-linear uncertain polynomial with interval uncertainty. The proposed control framework of this study facilitates implementing the controller design theories to find the appropriate feedback gain that can guarantee reaching to the desired system states. This can be translated as finding the sizes of CSs that can keep the waiting time (system state) below a threshold level.

A few definitions and preliminary results are reviewed first to demonstrate the transforming of EV sizing problem to the problem of analysing the robust stability of an interval uncertain polynomial. The Kharitanov theorem is the bedrock of the analysis in this paper. It deals with the robust stability of interval uncertain polynomials. Two solutions will be presented for CS sizing based on i) zero exclusion condition for Kharitonov polynomials, and 2) zero exclusion condition for a polytop of closed loop polynomials.

Definition 5: A family of uncertain polynomials given by $\mathcal{P} = \{p(.,q) : q \in Q\}$ *is said to have invariant degree if for any* $q^1, q^2 \in Q$ *it follows that* $\deg p(s,q^1) = \deg p(s,q^2)$.

Definition 6: A set $C \subseteq \mathbf{R}^k$ *is convex if the line joining any two points it contains the whole line segment joining them. Mathematically, for any given* $c_1, c_2 \in C$ *and* $\lambda \in [0,1]$ *we have* $\lambda C_1 + (1-\lambda)c_2 \in C$. *The convex hull of a shape denoted by* conv$\{.\}$ *is the smallest convex set that contains it.*

Definition 7: A family of polynomials $\mathcal{P} = \{p(.,q) : q \in Q\}$ *is an interval polynomial family if p has an independent uncertainty structure, meaning that each coefficient of p continuously depends on q and Q is a convex box.*

Definition 8: Given a family of polynomials $\mathcal{P} = \{p(.,q) : q \in Q\}$, *the value set at* $z \in \mathbf{C}$ *is the image of Q under* $p(z,.)$ *and is given by* $p(z,Q) = \{p(z,q) : q \in Q\}$.

Theorem 9: [15] For the interval polynomial family $\mathcal{P} = \{p(.,q) : q \in Q\}$ *with* $p(s,q)$ *where its coefficients continuously depend on q, there exists a second interval polynomial family* $\tilde{\mathcal{P}} = \{\tilde{p}(.,\tilde{q}) : \tilde{q} \in \tilde{Q}\}$ *with* $\tilde{p}(.,\tilde{q})$ *in the form of* $\tilde{p}(.,\tilde{q}) = \sum_{i=0}^{n} \tilde{q}_i s^i$ *and, moreover,* $\tilde{\mathcal{P}} = \mathcal{P}$.

Using the above theorem, known as lumping theorem, the uncertain polynomial can be written as $p(s,q) = \sum_{i=0}^{n} q_i s^i$ and subsequently, the interval family can be described by $p(s,q) = \sum_{i=0}^{n}[q_i^-, q_i^+]s^i$ where q_i^- and q_i^+ denote the extreme points of the bound of uncertainty q_i.

Definition 10 [15]: The four Kharitonov polynomials associated with the interval polynomial $p(s,q) = \sum_{i=0}^{n}[q_i^-, q_i^+]s^i$ *are the four fixed polynomials*

$$K_1(s) = q_0^- + q_1^- s + q_2^+ s^2 + q_3^+ s^3 + q_4^- s^4 + q_5^- s^5 + q_6^+ s^6 + \dots$$
$$K_2(s) = q_0^+ + q_1^+ s + q_2^- s^2 + q_3^- s^3 + q_4^+ s^4 + q_5^+ s^5 + q_6^- s^6 + \dots$$
$$K_3(s) = q_0^+ + q_1^- s + q_2^- s^2 + q_3^+ s^3 + q_4^+ s^4 + q_5^- s^5 + q_6^- s^6 + \dots$$
$$K_4(s) = q_0^- + q_1^+ s + q_2^+ s^2 + q_3^- s^3 + q_4^- s^4 + q_5^+ s^5 + q_6^+ s^6 + \dots.$$

Now, we present the Kharitonov Theorem on robustness of interval polynomials.

Theorem 11 [15]: An interval polynomial family $\mathcal{P}$ *with invariant degree is robustly stable if and only if its four Kharitonov polynomials, or Kharitonov rectangles, are stable.*

The above theorem can be graphically tested using the zero exclusion condition as stated below.

Lemma 12: Given an interval family $\mathcal{P} = \{p(.,q) : q \in Q\}$ *with invariant degree and at least one stable member* $p(s,q^0)$, $\mathcal{P}$ *is robustly stable if and only if* $z = 0$ *is excluded from the kharitonov rectangle at all non-negative frequencies; i.e.,* $0 \notin p(j\omega, Q)$ *for all frequencies* $\omega \geq 0$.

The calculation of the value set for the whole range of frequencies is computationally inefficient. However, there is a cutoff frequency $\omega_c > 0$ such that $0 \notin p(j\omega, Q)$ for all $\omega \geq \omega_c$. This means that the computation of the value set can be terminated at ω_c. The existance of ω_c is established in [15] using the invariant degree condition. It follows that the cutoff frequency can be calculated from

$$\omega_c = 1 + \frac{\max\{q_0^+, q_1^+, \dots, q_{n-1}^+\}}{q_n^-} \tag{8}$$

Theorem 11 and Lemma 12 can be used to find the solution of CS sizing problem. As indicated in example 2, the closed loop polynomial of each subgraph of the CS network is an interval uncertain polynomial which can be over-bounded to attain an affine-linear uncertain polynomial. Proposition below summarize the result using the Kharitonov rectangle and zero exclusion condition.

Proposition 13: (First Proposed Solution to CS Sizing). For a given subgraph $\mathcal{S}_i$ *attained from partitioning of the CS network featuring only one CS with capacity k, the states T of the associated transfer function computed from (7) can reach the desired waiting time in finite time if* $z = 0$ *is excluded from the the kharitonov rectangles of the affine-linear polynamial* $D(s) + k.N(s)$ *with invariant degree for* $0 \leq \omega \leq \omega_c$.

Proof: The proof simply follows from the results of Theorem 11 and lemma 12 with the closed loop poynomial of the subgraph attained from $D(s) + k.N(s)$. □

The proposition above is tested for the Tesla CS network of Sydney, Australia and satisfactory results are attained in Section III. Now, we proceed with the second solution to CS sizing using a more general form of uncertainty.

Definition 14: A set $X \subseteq R^k$ *is said to be pathwise connected if for any two points* $x_0, x_1 \in X$, *there is a continuous function* $\Phi : [0,1] \to X$ *such that* $\Phi(0) = x_0$ *and* $\Phi(1) = x_1$.

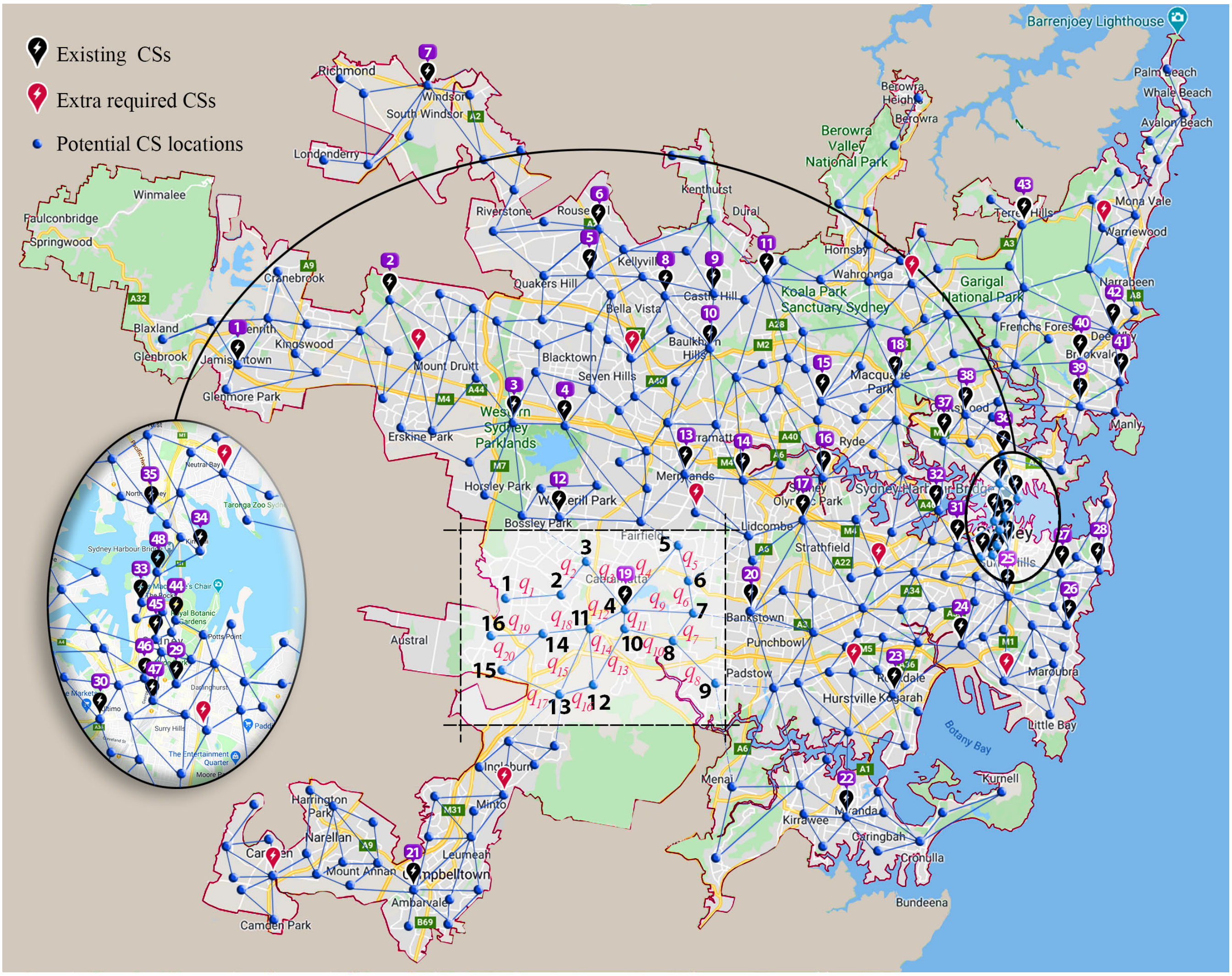

FIGURE 3. Tesla CS map of Sydney, Australia [18] used for simulations. The black, red, and blue location icons correspond to the nodes with existing CSs, new CSs (determined in this paper), and the potential CS locations, respectively.

Every convex set of uncertainty is thus pathwise connected. Obviously, the uncertainty in the traffic map is also pathwise connected as it is a convex set.

Theorem 15 [15]: Let the family of invariant degree polynomials $\mathcal{P} = \{p(., q) : q \in Q\}$ with cutoff frequency ω_c and uncertainty bounding set Q, which is pathwise connected, have continuous coefficient functions $a_i(q)$ for $i = 0, 1, 2, \ldots, n$ and at least one stable member $p(s, q^0)$. Then $\mathcal{P}$ is robustly stable if and only if the origin $z = 0$ is excluded from the value set $p(j\omega, Q)$ at all frequencies $\omega \geq 0$; i.e., $\mathcal{P}$ is robustly stable if and only if $0 \notin p(j\omega, Q)$ for all frequencies $\omega \geq 0$.

Now the value sets for a polytop of polynomials can be defined. It is argued in [15] that the related value sets are polygons in the complex plane. A polygonal property of value sets for a plytop of polynomials is presented below which facilitates testing the zero exclusion condition.

Lemma 16 [15]: Given a polytop of polynomials $\mathcal{P} = \{p(., q) : q \in Q\}$ with uncertainty bounding set $Q = conv\{q^i\}$, for fixed $z \in \mathbf{C}$, the value set $p(z, Q)$ is a polygon with generating set $\{p(z, q^i)\}$ or $p(z, Q) = conv\{p(z, q^i)\}$. In addition, all edges of the polygon $p(z, Q)$ are obtained from the edges of Q so that if z_0 is a point on an edge of $p(z, Q)$, then $z_0 = p(z, q^0)$ for some q^0 is on an edge of Q.

The second solution to EV sizing problem is summarized in the proposition below.

Lemma 17: (Second Proposed Solution to CS Sizing) For a given subgraph $\mathcal{S}_i$ of the graph of CS network with capacity k, the states T of the associated transfer function computed from (7) can reach to the desired waiting time in finite time if $z = 0$ is excluded from the value set $D(j\omega, Q) + k.N(j\omega, Q)$ for all frequencies $\omega \geq 0$.

Proof: The proof is a straightforward result of theorem 15 and lemma 16 with the closed loop polynomial of the subgraph attained from $D(s) + k.N(s)$. $\square$

The above proposition gives a solution to the sizing of each CS in each subgraph. A clear cut solution to the CS placement and sizing is presented in Algorithm 1.

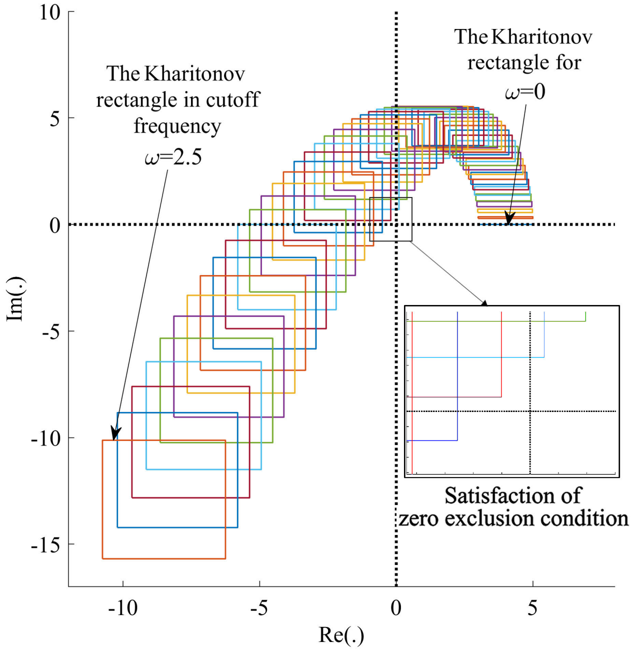

FIGURE 4. The Kharitonov rectangles for the subgraph shown in Figure 3.

Algorithm 1 The Proposed Graph-Based Solutions to the Robust CS Placement and Sizing Problem in EV Networks

Input: The maximum and minimum number of EVs arriving at each CS during its operation.

Output: The locations of extra required CSs and sizes of all (existing and new) CSs.

1: **while** maximum iteration is not met **do**
2: Calculate S_{CS} from (4).
3: Apply partitioning algorithm to EV network to drive N_D subgraphs featuring one driver node per partition.
4: **for** $i = 1$ to N_D **do**
5: Compute the cutoff frequency ω_c^i from (8).
6: Investigate the zero exclusion condition of Lemma 12 for $0 \leq \omega \leq \omega_c^i$ and a fixed k using one of the Proposition 13 or Lemma 17.
7: **if** the zero exclusion condition is satisfied **then** the size of CS is k.
8: **else**
Increase k and go to step 6.
9: **end if**
10: **end for**
11: **end while**

III. IMPLEMENTATION OF PROPOSED CS PLACEMENT AND SIZING STRATEGY IN TESLA CS NETWORK OF SYDNEY

The proposed approaches of this paper (summarized in Algorithm 1) are applied on the Tesla CS network of Sydney [18] illustrated in Figure 3. The 48 existing Tesla charging stations are demonstrated in Figure 3 with black location icons.

TABLE 1. Number of connectors N_C, the size of each existing CS $|S_{SC}|_i$ in kW, and the size of each CS in kW after expansion $|S_{SC}|_i$ of Tesla CS network of Sydney.

CS	N_C	$\lvert S^0_{CS}\rvert_i$	$\lvert S_{CS}\rvert_i$	CS	N_C	$\lvert S^0_{CS}\rvert_i$	$\lvert S_{CS}\rvert_i$
Existing CSs with Present and Calculated New Sizes							
1	2	22	138	2	1	22	84
3	4	44	79	4	1	22	93
5	3	22	84	2	6	22	142
7	2	6	118	8	1	5	162
9	3	22	98	10	2	27	145
11	2	22	89	12	2	22	126
13	2	22	122	14	4	44	75
15	2	7	110	16	5	44	96
17	4	44	120	18	2	3	123
19	3	22	95	20	4	26	143
21	2	22	120	22	2	22	78
23	2	6	117	24	4	29	86
25	4	44	116	26	2	22	145
27	4	22	68	28	2	22	128
29	2	4	126	30	3	22	98
31	2	22	78	32	3	22	129
33	5	44	93	34	2	22	136
35	3	22	85	36	1	22	124
37	3	5.2	110	38	1	6	96
39	4	44	158	40	4	22	85
41	4	22	103	42	1	22	73
43	2	22	134	44	2	22	79
47	2	22	106	48	4	28	112
Additional CSs with Calculated Sizes							
49	-		94	50	-		129
51	-		87	52	-		85
53	-		115	54	-		95
55	-		134	56	-		113
57	-		105	58	-		93
59	-		84	60	-		138
Summary and Comparison of Results							
Existing Tesla CSs				**Upgraded Tesla CSs**			
Total Number of CSs: 48				Total Number of CSs: 60			
Total S Size: 1054.4 kW				Total S Size: 5025 kW			

All CSs are equipped with the standard DC fast chargers with the service time of $10 - 15$ minutes. According to Energeia Analysis, with current uptake rate of EVs, the number of EVs in Sydney by the year 2025 will be increased by about %500 [19]. The graph of this network is augmented in Figure 3 considering the variable traffic flow in 2025.

The number of connectors and sizes of existing CSs are indicated in Table 1. The extra required CSs (S_{CS}) are calculated by following the modified maximum matching (Lemma 2) principle as explained in Lemma 17. Since the result of maximum matching is a set of unmatched nodes that must be considered as CSs, we have performed it on a modified map where the nodes are selected in locations where it is practical to construct CS infrastructure. This has led to a set of 12 unmatched nodes (indicated by red location symbol in Figure 3) in addition to 48 existing CSs which are pre-set as unmatched. The resulted extra CSs are illustrated in Figure 3. Having the set S_{CS}, we can proceed with computing the size of each CS after constructing the graph of CS network and partitioning it into $|S_{CS}|$ subgraphs. Due

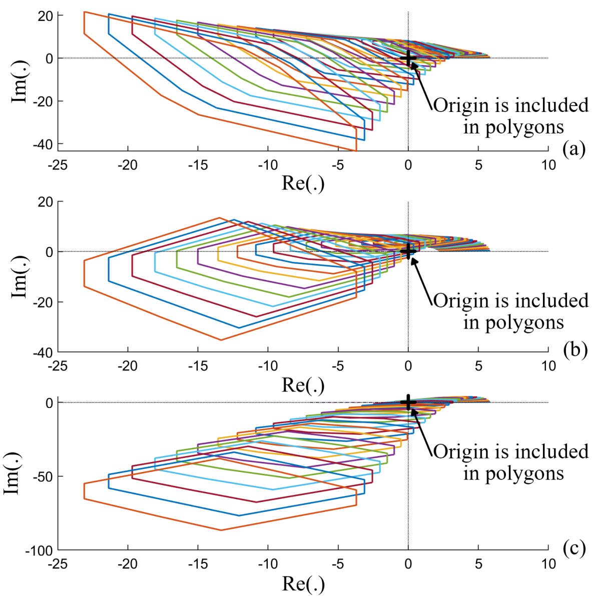

FIGURE 5. The zero exclusion condition for the polygonal polynomials of subgraph shown in Figure 3 for (a) $k = 65$, (b) $k = 75$, (c) and $k = 85$.

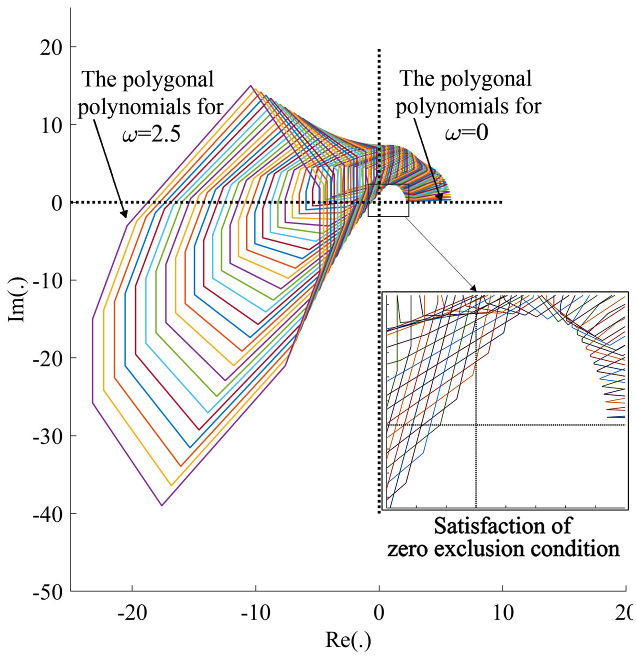

FIGURE 6. The zero exclusion condition for the polygonal polynomials of subgraph shown in Figure 3 for $k = 95$.

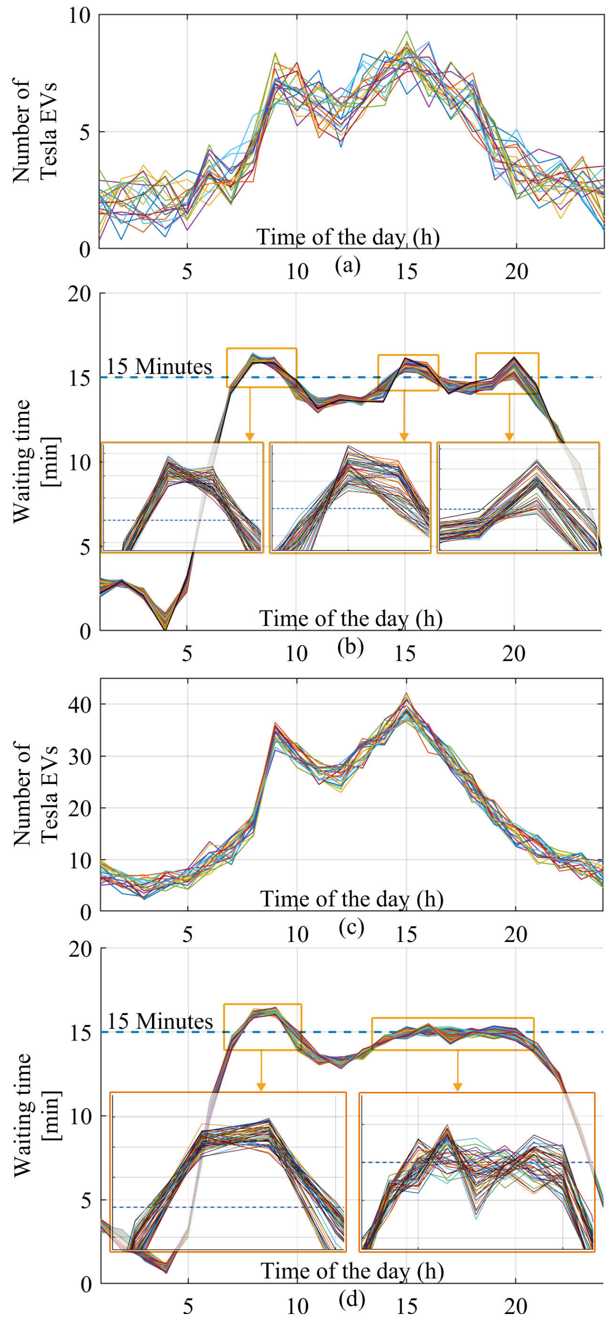

FIGURE 7. (a) The traffic flow of the existing network with 48 CSs (represented by black icons in Figure 3), (b) the corresponding waiting time of the existing 48 CSs, (c) The traffic flow of the expanded network (in year 2025), and (d) The corresponding waiting times of 48 pre-existing and 12 extra added CSs (represented by red icons in Figure 3).

to space limitation, here the simulation results for only one of the subgraphs (the area separated with a dashed rectangle in Figure 3) are presented. The weights on the edges of this subgraph represent the variable traffic flow q_i between two nodes. The system has 16 nodes and 20 edges. The number of nodes and edges indicate the order of subgraph and the number of uncertainties, respectively. The order of system is 16 and as such, it is a big transfer function with very long coefficients $a_i(q)$ depending on Q. Here, only the state space representation of the subgraph is presented. The adjacency matrix $\mathcal{A}$ for the subgraph is the equation can be derived, as shown at the bottom of next page.

where the zeros are represented with dots for clarity. The input matrix is $B = \ldots 1 \ldots\ldots\ldots^T$ and $C = \mathbf{1}$. By computing the transfer function of this subgraph and constructing $D(s) + k.N(s)$, the two proposed methods for calculating

$$
\begin{bmatrix}
q_{ii} & q_1 & \cdot & \cdot & \cdot & \cdot & \cdot & \cdot & \cdot & \cdot & \cdot & \cdot & \cdot & \cdot & \cdot & \cdot \\
q_1 & q_{ii} & q_2 & \cdot & \cdot & \cdot & \cdot & \cdot & \cdot & \cdot & \cdot & \cdot & \cdot & \cdot & \cdot & \cdot \\
\cdot & q_2 & q_{ii} & q_3 & \cdot & \cdot & \cdot & \cdot & \cdot & \cdot & \cdot & \cdot & \cdot & \cdot & \cdot & \cdot \\
\cdot & \cdot & q_3 & q_{ii} & q_4 & \cdot & q_9 & \cdot & \cdot & q_{11} & q_{12} & \cdot & \cdot & \cdot & \cdot & \cdot \\
\cdot & \cdot & \cdot & q_4 & q_{ii} & q_5 & \cdot & \cdot & \cdot & \cdot & \cdot & \cdot & \cdot & \cdot & \cdot & \cdot \\
\cdot & \cdot & \cdot & \cdot & q_5 & q_{ii} & q_6 & \cdot & \cdot & \cdot & \cdot & \cdot & \cdot & \cdot & \cdot & \cdot \\
\cdot & \cdot & \cdot & q_9 & \cdot & q_6 & q_{ii} & q_7 & \cdot & \cdot & \cdot & \cdot & \cdot & \cdot & \cdot & \cdot \\
\cdot & \cdot & \cdot & \cdot & \cdot & \cdot & q_7 & q_{ii} & q_8 & q_{10} & \cdot & \cdot & \cdot & \cdot & \cdot & \cdot \\
\cdot & \cdot & \cdot & \cdot & \cdot & \cdot & \cdot & q_8 & q_{ii} & \cdot & \cdot & \cdot & \cdot & \cdot & \cdot & \cdot \\
\cdot & \cdot & \cdot & q_{11} & \cdot & \cdot & \cdot & q_{10} & \cdot & q_{ii} & \cdot & q_{13} & \cdot & \cdot & \cdot & \cdot \\
\cdot & \cdot & \cdot & q_{12} & \cdot & \cdot & \cdot & \cdot & \cdot & \cdot & q_{ii} & q_{14} & q_{15} & q_{18} & \cdot & \cdot \\
\cdot & \cdot & \cdot & \cdot & \cdot & \cdot & \cdot & \cdot & \cdot & q_{13} & q_{14} & q_{ii} & q_{16} & \cdot & \cdot & \cdot \\
\cdot & \cdot & \cdot & \cdot & \cdot & \cdot & \cdot & \cdot & \cdot & \cdot & q_{15} & q_{16} & q_{ii} & \cdot & q_{17} & \cdot \\
\cdot & \cdot & \cdot & \cdot & \cdot & \cdot & \cdot & \cdot & \cdot & \cdot & q_{18} & \cdot & \cdot & \cdot q_{ii} & q_{20} & q_{19} \\
\cdot & \cdot & \cdot & \cdot & \cdot & \cdot & \cdot & \cdot & \cdot & \cdot & \cdot & \cdot & q_{17} & q_{20} & q_{ii} & \cdot \\
\cdot & \cdot & \cdot & \cdot & \cdot & \cdot & \cdot & \cdot & \cdot & \cdot & \cdot & \cdot & \cdot & q_{19} & \cdot & q_{ii}
\end{bmatrix}
$$

the size of the CS at node 4 are implemented by graphical examining of zero exclusion condition (Figures 4-7 and Table 1). Note that node 19 in the subgraph is re-numbered as node 4.

The cutoff frequency for this subgraph is calculated using (8) as $\omega_c = 2.5$. The zero exclusion condition for $k = 95$ and $0 \leq \omega \leq 2.5$ is investigated in MATLAB and the result is demonstrated in Figure 4 for 125 equally spaced frequencies. Clearly, the origin of the complex plane is excluded from the rectangles of Kharitonov and, as such, the associated CS can handle the demand by increasing its capacity to 95kW.

Proceeding with Lemma 17 will lead to the similar results as Kharitanov rectangles. To this end, we have examined the zero exclusion condition of Lemma 17 for three values of k less than 95. The results are shown in Figures 5.(a)-(c). As indicated in these figures, the origin of complex plane is included in the polygons for all three values of k. The subgraph is re-examined with $k = 95$ and, as shown in Figure 6, zero is excluded from the polygons. There are 20 uncertainties but the attained polygons are not 20-sided as most of extreme points fall inside the convex hull of the polynomial for extreme points. The capacity of the rest of CSs are computed in a same way and the results are presented in Table 1. Finally, the waiting time of node 19 is calculated in MATLAB for the variable traffic during 24 hours (as shown in Figure 7.(a)) and the result indicated in Figure 7.(b) shows that the waiting time is maintained near or lower than the 15 minutes threshold at all times.

IV. CONCLUSION

This study proposes novel graph theoretic solutions from the lens of control theories to address the CS placement and sizing in EV networks with dynamic traffic flow. The new CS placement approach considers the placement of required extra CSs for an expanding EV network with existing stations. It is accomplished by modifying the maximum matching principle to find the set of extra required CSs. Subsequently, the CS sizing is addressed by resizing the existing stations in addition to the sizing of new required CSs. The sizing is performed by transforming the problem of CSs sizing for a network with dynamic traffic to the problem of robust stability of a family of polynomials with affine-linear interval uncertainties where each uncertain parameter represents an uncertain interval number of EVs in the zone between two nearby nodes. In addition to dynamic traffic flow consideration, the approach is unique as it relies on more analytical methodologies compared with the conventional solutions to CS placement and sizing problem that often suffer from computational issues such as conservative responses or intractable solutions. On the other hand, the fast growing of electric vehicles (EVs) deployment necessitates expanding the current charging stations (CSs) networks. Nearly all previous studies on CS placement and sizing are focused on the planning and design of EV networks with no existing stations. The proposed approach of this study, however, addresses the placement of new and extra required CSs as well as re-sizing of existing CSs for expanded network.

The proposed graph theoretic approaches are implemented and verified on the existing Tesla CS Network of Sydney, Australia assuming an increase of 500% in EV traffic by year 2025. Detailed simulation results indicate that the average waiting times during peak hours at CSs are kept near 15 minutes for upgraded EV network with +500% increase in EV traffic, 60 CSs, and total charging capacity of 5.025 MW.

REFERENCES

[1] Y. Li, C. Rehtanz, S. Ruberg, L. Luo, and Y. Cao, "Assessment and choice of input signals for multiple HVDC and FACTS wide-area damping controllers," *IEEE Trans. Power Syst.*, vol. 27, no. 4, pp. 1969–1977, Nov. 2012, doi: 10.1109/TPWRS.2012.2189865.

[2] Z. Moghaddam, I. Ahmad, D. Habibi, and M. A. S. Masoum, "A coordinated dynamic pricing model for electric vehicle charging stations," *IEEE Trans. Transp. Electrific.*, vol. 5, no. 1, pp. 226–238, Mar. 2019, doi: 10.1109/TTE.2019.2897087.

[3] X. Zhao, X. Zhao, Q. Yu, Y. Ye, and M. Yu, "Development of a representative urban driving cycle construction methodology for electric vehicles: A case study in Xi'an," *Transp. Res. D, Transp. Environ.*, vol. 81, Apr. 2020, Art. no. 102279, doi: 10.1016/j.trd.2020.102279.

[4] M. P. Anand, B. Bagen, and A. Rajapakse, "Probabilistic reliability evaluation of distribution systems considering the spatial and temporal distribution of electric vehicles," *Int. J. Electr. Power Energy Syst.*, vol. 117, May 2020, Art. no. 105609, doi: 10.1016/j.ijepes.2019.105609.

[5] S. R. Gampa, K. Jasthi, P. Goli, D. Das, and R. C. Bansal, "Grasshopper optimization algorithm based two stage fuzzy multiobjective approach for optimum sizing and placement of distributed generations, shunt capacitors and electric vehicle charging stations," *J. Energy Storage*, vol. 27, Feb. 2020, Art. no. 101117, doi: 10.1016/j.est.2019.101117.

[6] Y. Zhang, Q. Zhang, A. Farnoosh, S. Chen, and Y. Li, "GIS-based multi-objective particle swarm optimization of charging stations for electric vehicles," *Energy*, vol. 169, pp. 844–853, Feb. 2019, doi: 10.1016/j.energy.2018.12.062.

[7] L. T. Al-Bahrani, B. Horan, M. Seyedmahmoudian, and A. Stojcevski, "Dynamic economic emission dispatch with load dema nd management for the load demand of electric vehicles during crest shaving and valley filling in smart cities environment," *Energy*, vol. 195, Mar. 2020, Art. no. 116946, doi. 0.1016/j.energy.2020.116946.

[8] C. Doppstadt, A. Koberstein, and D. Vigo, "The hybrid electric vehicle—Traveling salesman problem with time windows," *Eur. J. Oper. Res.*, vol. 253, no. 3, pp. 675–692, 2020, doi: 10.1016/j.ejor.2019.12.031.

[9] M.-W. Tian, S.-R. Yan, X.-X. Tian, M. Kazemi, S. Nojavan, and K. Jermsittiparsert, "Risk-involved stochastic scheduling of plug-in electric vehicles aggregator in day-ahead and reserve markets using downside risk constraints method," *Sustain. Cities Soc.*, vol. 55, Apr. 2020, Art. no. 102051, doi: 10.1016/j.scs.2020.102051.

[10] X. Lü, Y. Wu, J. Lian, Y. Zhang, C. Chen, P. Wang, and L. Meng, "Energy management of hybrid electric vehicles: A review of energy optimization of fuel cell hybrid power system based on genetic algorithm," *Energy Convers. Manage.*, vol. 205, Feb. 2020, Art. no. 112474, doi: 10.1016/j.enconman.2020.112474.

[11] J. Li and B. Yang, "Analysis of greenhouse gas emissions from electric vehicle considering electric energy structure, climate and power economy of ev: A China case," *Atmos. Pollut. Res.*, vol. 11, no. 6, pp. 1–11, Jun. 2020, doi: 10.1016/j.apr.2020.02.019.

[12] H. Liu and D. Z. W. Wang, "Locating multiple types of charging facilities for battery electric vehicles," *Transp. Res. B, Methodol.*, vol. 103, pp. 30–55, Sep. 2017, doi: 10.1016/j.trb.2017.01.005.

[13] M. E. Kabir, C. Assi, H. Alameddine, J. Antoun, and J. Yan, "Demand aware deployment and expansion method for an electric vehicles fast charging network," in *Proc. IEEE Int. Conf. Commun., Control, Comput. Technol. Smart Grids (SmartGridComm)*, Oct. 2019, pp. 1–7, doi: 10.1109/SmartGridComm.2019.8909746.

[14] H. Parastvand, V. Moghaddam, O. Bass, M. A. S. Masoum, A. Chapman, and S. Lachowicz, "A graph automorphic approach for placement and sizing of charging stations in EV network considering traffic," *IEEE Trans. Smart Grid*, early access, Apr. 3, 2020, doi: 10.1109/TSG.2020.2984037.

[15] B. R. Barmish, *New Tools for Robustness of Linear Systems*. vol. 195, 1st ed. New York, NY, USA: Macmillan Coll Div, 1993, pp. 844–853.

[16] H. Parastvand and M.-J. Khosrowjerdi, "Parameterised controller synthesis for SISO-LTI uncertain plants using frequency domain information," *Int. J. Syst. Sci.*, vol. 47, no. 1, pp. 32–44, Jan. 2016, doi: 10.1080/00207721.2015.1022026.

[17] G. Agnarsson and R. Greenlaw, "Graph theory: Modeling, applications, and algorithms," in *Atmospheric Pollution Research*, 1st ed. London, U.K.: Pearson, 2006.

[18] (May 2020). *The Network of Tesla Charging Stations*. [Online]. Available: https://www.tesla.com/en_AU/findus

[19] *Australian Electric Vehicle Market Study*, Prepared by ENERGEIA for ARENA and CEFC, Sydney, NSW, Australia, 2018.

[20] C. Ocampo-Martinez, S. Bovo, and V. Puig, "Partitioning approach oriented to the decentralised predictive control of large-scale systems," *J. Process Control*, vol. 21, no. 5, pp. 775–786, Jun. 2011, doi: 10.1016/j.jprocont.2010.12.005.

[21] Y. Yang and G. Xie, "Mining maximum matchings of controllability of directed networks based on in-degree priority," in *Proc. 35th Chin. Control Conf. (CCC)*, Jul. 2016, pp. 1263–1267, doi: 10.1109/ChiCC.2016.7553261.

[22] Y. Liu, J. J. Slotine, and A. L. Barabási, "Controllability of complex networks," *Nature*, vol. 473, pp. 167–173, May 2011.

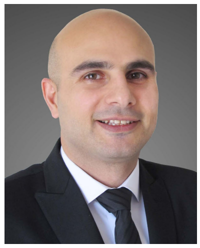

HOSSEIN PARASTVAND (Student Member, IEEE) received the B.S. degree in instrumentation and control from the Shiraz University of Technology, Shiraz, Iran, in 2008, and the M.S. degree in control engineering from the Sahand University of Technology, Tabriz, Iran, in 2010. He is currently pursuing the Ph.D. degree with the Smart Energy Systems Group, Edith Cowan University, Joondalup, WA, Australia. From 2010 to 2017, he was a Senior Automation and Control Engineer with MegaTrans Company, Iran. His main research interests include control theory and its application in power networks and smart grid.

OCTAVIAN BASS (Senior Member, IEEE) graduated from the Politehnica University of Timisoara, Romania, in 1995. He received the Ph.D. degree from the Politehnica University of Timisoara, in 2001. His employment history includes research positions at the Budapest University of Technology and Economics, Hungary, The Hong Kong Polytechnic University, Hull University, U.K., and Utsunomiya University, Japan. He was a Lecturer with James Cook University, Australia, from 2006 to 2009. He is currently a Senior Lecturer with the School of Engineering, Edith Cowan University, Perth, Australia. He has coauthored 90 professional publications. His research interests include smart grid technologies, renewable energy resources, and non-linear dynamics in power electronics.

MOHAMMAD A. S. MASOUM (Senior Member, IEEE) received the B.S. and M.S. degrees from the University of Colorado, Denver, CO, USA, in 1983 and 1985, respectively, and the Ph.D. degree from the University of Colorado, Boulder, CO, USA, in 1991, all in electrical and computer engineering. He was an Associate Professor with the Iran University of Science and Technology, Tehran, Iran, from 1993 to 2003, and a Professor with Curtin University, Perth, Australia, from 2004 to 2018. He is currently an Associate Professor with the Department of Engineering, Utah Valley University, Orem, UT, USA. He has coauthored *Power Quality in Power Systems and Electrical Machines* (Elsevier, 2008 and 2015) and *Power Conversion of Renewable Energy Systems* (Springer, 2011 and 2012). He is an Editor of the IEEE Transactions on Smart Grid and the IEEE Power Engineering Letters.

AIRLIE CHAPMAN (Senior Member, IEEE) received the B.S. degree in aeronautical engineering and the M.S. degree in engineering research from the University of Sydney, Australia, in 2006 and 2008, respectively, and the M.S. degree in mathematics and the Ph.D. degree in aeronautics and astronautics from the University of Washington, Seattle, in 2013. She is currently a Senior Lecturer with the Department of Mechanical Engineering, The University of Melbourne. Her research interests are multi-agent dynamics, networked dynamic systems, data-driven control, and graph theory with applications to robotics and aerospace systems.

STEFAN W. LACHOWICZ (Senior Member, IEEE) received the M.Eng.Sc. and Ph.D. degrees in electronic engineering from the Lodz University of Technology, Lodz, Poland, in 1981 and 1986, respectively. From 1992 to 1994, he was a Research Assistant and an Assistant Professor with the Institute of Electronics, Lodz University of Technology. He has been a Lecturer and a Senior Lecturer with the School of Engineering, Edith Cowan University, Perth, WA, Australia, since 1993 and 2001, respectively. He has authored or coauthored about 110 research articles. His current research interests include modern power systems, smart energy systems, electric vehicles, and power electronics.